Biochimica et Biophysica Acta 1852 (2015) 2712–2721

Contents lists available at ScienceDirect

Biochimica et Biophysica Acta

journal homepage: www.elsevier.com/locate/bbadis

Functional analysis of splicing mutations in the *IDS* gene and the use of antisense oligonucleotides to exploit an alternative therapy for MPS II

Liliana Matos [a,b], Vânia Gonçalves [c], Eugénia Pinto [d], Francisco Laranjeira [d], Maria João Prata [b,e], Peter Jordan [c], Lourdes R. Desviat [f,g,h], Belén Pérez [f,g,h,1], Sandra Alves [a,*,1]

[a] Research and Development Unit, Department of Human Genetics, INSA, Porto, Portugal
[b] Department of Biology, Faculty of Sciences, University of Porto, Porto, Portugal
[c] Research and Development Unit, Department of Human Genetics, INSA, Lisbon, Portugal
[d] Biochemical Genetics Unit, Center for Medical Genetics Jacinto Magalhães, Porto Hospital Center, Porto, Portugal
[e] i3S - Instituto de Investigação e Inovação em Saúde/IPATIMUP - Institute of Molecular Pathology and Immunology of the University of Porto, Porto, Portugal
[f] Centro de Diagnóstico de Enfermedades Moleculares, Centro de Biología Molecular Severo Ochoa, UAM-CSIC, Universidad Autónoma de Madrid, Madrid, Spain
[g] CIBER de Enfermedades Raras (CIBERER), Madrid, Spain
[h] IDIPaz, Madrid, Spain

ARTICLE INFO

Article history:
Received 10 April 2015
Received in revised form 16 September 2015
Accepted 21 September 2015
Available online 25 September 2015

Keywords:
Lysosomal storage disorders
IDS gene
Splicing regulation
Antisense therapy

ABSTRACT

Mucopolysaccharidosis II is a lysosomal storage disorder caused by mutations in the *IDS* gene, including exonic alterations associated with aberrant splicing. In the present work, cell-based splicing assays were performed to study the effects of two splicing mutations in exon 3 of *IDS*, i.e., c.241C>T and c.257C>T, whose presence activates a cryptic splice site in exon 3 and one in exon 8, i.e., c.1122C>T that despite being a synonymous mutation is responsible for the creation of a new splice site in exon 8 leading to a transcript shorter than usual. Mutant minigene analysis and overexpression assays revealed that SRSF2 and hnRNP E1 might be involved in the use and repression of the constitutive 3′ splice site of exon 3 respectively. For the c.1122C>T the use of antisense therapy to correct the splicing defect was explored, but transfection of patient fibroblasts with antisense morpholino oligonucleotides (n = 3) and a locked nucleic acid failed to abolish the abnormal transcript; indeed, it resulted in the appearance of yet another aberrant splicing product. Interestingly, the oligonucleotides transfection in control fibroblasts led to the appearance of the aberrant transcript observed in patients' cells after treatment, which shows that the oligonucleotides are masking an important *cis*-acting element for 5′ splice site regulation of exon 8. These results highlight the importance of functional studies for understanding the pathogenic consequences of mis-splicing and highlight the difficulty in developing antisense therapies involving gene regions under complex splicing regulation.

1. Introduction

Mucopolysaccharidosis type II (MPS II, Hunter syndrome, OMIM# 309900) is an X-linked, recessive, lysosomal storage disorder (LSD) caused by mutations in the *IDS* gene (OMIM* 300823). *IDS* codes for the enzyme iduronate-2-sulfatase (IDS, EC 3.1.6.13), which is required for the degradation of the glycosaminoglycans dermatan and heparan sulfate. The progressive abnormal storage of these compounds within the lysosomes leads to the eventual malfunction of different organs and systems [1]. Although two clinical forms, mild and severe, are generally recognized in MPS II, they are just the ends of a wide spectrum of clinical severity, likely related to the diversity of mutations affecting the *IDS* gene [1].

IDS is located on chromosome Xq28 and spans nine exons [2]. About 20 kb telomeric to the functional gene lies a functional pseudogene showing homology with exons 2 and 3 and introns 2, 3 and 7 [3-5]. More than 500 MPS II causal mutations have been reported in *IDS*, of which around 9% are single nucleotide substitutions that affect splice site signals (www.hgmd.org; [6]). However, this figure is probably an underestimate since the direct analysis of mRNA is not routinely performed in the diagnostic setting. Thus, the impact of missense, nonsense and synonymous mutations involved in the downregulation of splicing

Abbreviations: AMO, antisense morpholino oligonucleotide; AO, antisense oligonucleotide; C, healthy control; ESE, exonic splicing enhancer; ESS, exonic splicing silencer; hnRNP, heterogeneous nuclear ribonucleoprotein; ISE, intronic splicing enhancer; ISS, intronic splicing silencer; LNA, locked nucleic acid; LSD, lysosomal storage disorder; MPS II, mucopolysaccharidosis type II; NC, negative control; P, patient; siRNA, small interfering RNA; SR, arginine–serine; V, vector sequence; WT, wild-type.

* Corresponding author.
E-mail addresses: liliana.matos@insa.min-saude.pt (L. Matos), vania.goncalves@insa.min-saude.pt (V. Gonçalves), eugenia.pinto@chp.min-saude.pt (E. Pinto), francisco.laranjeira@chp.min-saude.pt (F. Laranjeira), mprata@ipatimup.pt (M.J. Prata), peter.jordan@insa.min-saude.pt (P. Jordan), lruiz@cbm.csic.es (L.R. Desviat), bperez@cbm.csic.es (B. Pérez), sandra.alves@insa.min-saude.pt (S. Alves).
[1] Co-last authors.

http://dx.doi.org/10.1016/j.bbadis.2015.09.011
0925-4439/

mechanisms may remain unknown; this is especially plausible for genes with a fine balance between constitutive and cryptic splice sites such as *IDS*, which requires the interaction of several auxiliary *cis*-acting elements for proper splicing to occur [7-9].

Splicing mutations can interfere with accurate pre-mRNA splicing if they affect nucleotides at (or in the vicinity of) acceptor (AG) or donor (GT) splice sites (detectable at the genomic DNA level). Correct consensus sequence recognition also relies on so-called exonic and intronic splicing enhancers (ESE and ISE) or silencers (ESS and ISS). These are usually bound by arginine–serine (SR) proteins and heterogeneous nuclear ribonucleoproteins (hnRNP) respectively. Regardless of their type (nonsense, missense or synonymous), single nucleotide mutations can interfere with all these internal splicing regulatory elements, causing partial or total exon skipping, intron retention, the creation of ectopic splice sites, and the activation of cryptic sites [7,10,11]. None of these effects can be deduced from the analysis of genomic DNA.

The understanding of basic splicing mechanisms is important if therapeutic strategies that might correct splicing defects are to be designed. Several studies have explored the potential of targeting aberrant pre-mRNA resulting from splicing mutations. These include the use of small molecule compounds that modulate alternative splicing, the overexpression or silencing of splice factors, *trans*-splicing approaches (spliceosome-mediated RNA *trans*-splicing, SMaRT), use of adapted U1 snRNAs complementary to the mutated site and antisense oligonucleotides used to correct mutation-induced aberrant splicing (Splice-switching oligonucleotides) or to redirect splicing to knock-down gene expression [12,13]. One of the most promising genetic therapies of this kind is pre-mRNA targeting by antisense oligonucleotides (AOs). These have been used to mask abnormal or cryptic splice sites and regulatory regions away from the mutated site aiming to restore pre-mRNA processing. AOs hybridize to a selected site in the pre-mRNA, and thus sterically hinder the recognition of a specific region by the spliceosomal machinery. The usage of the natural splice site(s) is thus promoted, recovering the production of normally spliced transcripts [14,15].

The modification of splicing by AOs has been shown effective in β-thalassemia (*HBB* gene) [16], ataxia-telangiectasia (*ATM* gene) [17,18], pyridoxine-dependent epilepsy (*ALDH7A1* gene) [19], hypomyelinating leukodystrophy (*PLP1* gene) [20], Niemann–Pick disease (*NPC1* gene) [21] and organic acidemias (*PCCA*, *PCCB* and *MUT* genes) [22,23]. AOs have also been used to modify alternative splicing in spinal muscular atrophy (*SMN2* gene) [24], and to target the pre-mRNA of genes involved in cancer such as *Bcl-x* [25] and *C-myc* [26,27]. Phenotypic improvements have been achieved using AOs *in vitro* and in animal models of Duchenne muscular dystrophy for which antisense therapy is now in the early phases of clinical trials [14,28].

In a previous study [29] involving Portuguese patients with MPS II, we detected several splicing mutations, some of which gave rise to alternative transcripts. Some involved exon 3 of *IDS*; the pre-mRNA region of this exon is particularly vulnerable to defects in splicing regulation. In the present work, functional analysis based on reporter minigenes was performed for two exon 3 nucleotide changes, c.257C>T [29-31] and c.241C>T [32], which confirmed these to be involved in exon 3 splicing dysregulation. Further, mutant minigene analysis and overexpression assays revealed that the SRSF2 (formerly SC35) and hnRNP E1 proteins might be involved in the use and repression of the constitutive 3′ splice site of exon 3 respectively.

Although enzyme replacement therapy is already available for MPS II, it has some serious limitations, justifying, therefore, the development of novel therapies for this disease. Hence, for MPS II patients' affected by splicing mutations, splicing therapeutics is a potential alternative or an adjunct therapeutic strategy. With this aim, tests were also performed to see whether AOs could be used to circumvent the effect of c.1122C>T [29,33], an exonic nucleotide change that creates a new 5′ splice site inside exon 8. The transfection of three antisense morpholino oligonucleotides (AMOs) and one locked nucleic acid (LNA) in patient fibroblasts did not abolish the abnormal transcript.

2. Material and methods

2.1. Patients and healthy individuals

Fibroblasts were obtained (during routine genetic analysis and under informed consent) from three male Portuguese patients - all carriers of one known mutation (Table 1) - with a biochemical diagnosis of MPS II, and from anonymous healthy donors. The confidentiality of personal data was respected at all times.

2.2. Cell culture and cycloheximide treatment of patients' fibroblasts

Fibroblasts, used as a source of mRNA and genomic DNA, were cultured following standard procedures in DMEM medium (Gibco Invitrogen, Carlsbad, USA) with 10% FBS and 1% kanamycin at 37 °C in a 5% CO_2 atmosphere.

To perform the nonsense-mediated mRNA decay (NMD) assays, fibroblast cells from Patient 1 (c.241C>T) and 2 (c.257C>T) were cultured in the presence of three different concentrations of cycloheximide (0.75, 1 and 2 mg/ml) for 6 h. Total RNA was then isolated and reverse-transcribed as described above. RT-PCR was performed using specific primers for exons 2 and 3 (Table I in [34]).

2.3. Molecular investigation

For molecular genetic analysis, genomic DNA was extracted automatically using a Bio Robot EZ1® system and the EZ1 DNA Tissue Extraction Kit (Qiagen, Hilden, Germany), following the manufacturer's instructions. Specific primers were used to amplify DNA fragments containing the nine exons of the *IDS* gene and their intronic flanking regions [29]. Total mRNA was isolated using the High Pure RNA Isolation Kit (Roche Applied Science, Indianapolis, USA) and reverse-transcribed using the "Ready-To-Go You-Prime First-Strand Beads" Kit (GE Healthcare, Buckinghamshire, UK), following the manufacturer's protocol. For RT-PCR, the specific primers shown in Table I [34] were designed using the Ensembl database (www.ensembl.org; Transcript: IDS-001 ENST00000340855). cDNA amplifications were performed in a total volume of 25 μl using the Hot-Start PCR Mastermix Immomix Red Kit (Bioline, London, UK), following the manufacturer's instructions, employing 0.2 μM of each primer and an annealing temperature of 60 °C (35 cycles). All PCR products were purified directly with Illustra ExoStar 1-Step™ (GE Healthcare, Buckinghamshire, UK), or after gel extraction using the Wizard® SV Gel and PCR Clean-Up System (Promega, Madison, USA). Sequencing reactions were then performed in an ABI Prism 3130xl genetic analyzer (Applied Biosystems, Foster City, USA). Sequencing profiles were compared with the *IDS* reference sequence ENSG00000010404 (www.ensembl.org) using the ClustalW2 bioinformatic tool (www.ebi.ac.uk/Tools/msa/clustalw2/).

2.4. Mutation nomenclature

The sequence used as reference for numbering the residues was the Ensembl sequence ENSG00000010404, and the mutation nomenclature was done in accordance with the recommendations of the Human Genome Variation Society (www.hgvs.org/mutnomen/).

2.5. Bioinformatic analysis

Prediction of the splicing scores for the natural, cryptic donor and acceptor splice sites was obtained using the *MaxEntScan* software: Maximum Entropy Model with ideal *MaxEnt* splice site scores of 11.81 for 5′ splice site and 13.59 for 3′ splice site (http://genes.mit.edu/burgelab/maxent/Xmaxentscan_scoreseq.html) [35]. Modeling of the

Table 1
Genotype and *in silico* analysis of genomic changes in the studied patients with mucopolysaccharidosis type II (MPS II).

Patient	cDNA change[a]	Protein change[a]	Mutation type	*In silico* effect of gDNA change[b]	Reference
1	c.241C>T	p.Q81X (CAA-TAA)	Nonsense/splicing	Reduction in splicing score for 3′ splice site (8.78 to 8.13)	Brusius-Facchin et al. [32] and present study
2	c.257C>T	p.P86L (CCG-CTG)	Missense/splicing	Creates an SRSF1 binding site and eliminates the hnRNP E1, hnRNP E2 and SRSF2 binding sites	Bunge et al. [30], Flomen et al. [31] and Alves et al. [29]
3	c.1122C>T	p.G374G (GGC-GGT)	Synonymous/ splicing	Increase in splicing score for 5′ splice site (7.46 to 9.22)	Popowska et al. [33] and Alves et al. [29]

[a] The mutation nomenclature is that recommended by HGVS. cDNA and protein numbering is based on the reference sequence in Ensembl (Ensembl sequence ENSG00000010404), taking nucleotide +1 as the A of the ATG translation initiation.
[b] *In silico* effect analyzed by *Splicing Rainbow* and *ESEfinder* 3.0 software.

alterations in exonic splicing enhancer or silencer sequences was performed using *ESEfinder* 3.0 (http://rulai.cshl.edu/cgi-bin/tools/ESE3/esefinder.cgi?process=home) [36,37] and *Splicing Rainbow* (http://www.ebi.ac.uk/asd) [38] software.

2.6. Minigene construction

For the *in vitro* splicing analysis of the variants c.241C>T and c.257C>T in *IDS* exon 3, the respective regions of patient and healthy control genomic DNA were amplified. Since an *IDS* pseudogene [3-5] exists that shows high homology with the *IDS* gene in the region corresponding to exons 2, 3 and introns 2 and 3, primers for these amplifications were designed to anneal at intron 1 and 3 in such a way that the amplified fragment matched the corresponding gene and not the pseudogene. A BamHI (Forward primer – Intron 1 BamHI F) and XhoI (Reverse primer - Intron 3 XhoI R) restriction enzyme cleavage site tail was added to each oligonucleotide (Table I in [34]). The PCR conditions were as described above. The fresh products were then subcloned into the TOPO vector (Invitrogen, Carlsbad, USA) following the manufacturer's protocol. The inserts were cut with BamHI and XhoI, and purified after gel excision. Using the Rapid Ligation Kit (Roche Applied Science, Indianapolis, USA) they were also cloned into pcDNA3.1-myc, a modified plasmid vector (Invitrogen, Carlsbad, USA) that contains the sequence for the Myc epitope (to be used as a sequence tag) upstream of the multiple cloning site (Fig. 1A in [34]).

To validate the in silico predicted changes in the splicing factors SRSF2 (formerly SC35), hnRNP E1 and hnRNP E2 (also known as α-CP1 or PCBP1 and α-CP2 or PCBP2) in the presence of the c.257C>T mutation, a mutant minigene was designed containing a small deletion (GCCCCGAGCC) in the mutated region which comprises the predicted *cis*-acting motifs for the binding of both mentioned *trans*-acting factors. The wild-type (WT) exon 3 minigene was used as template and the mutated minigene (ex3 del ESE/ESS motifs) was ordered from Nzytech (Lisbon, Portugal).

To functionally investigate the splicing defects caused by c.1122C>T in exon 8, wild-type and mutant minigenes were constructed in vector pSPL3 (Exon Trapping System, Life Technologies, Gibco, NY, USA), a specific vector for splicing analysis in which the multiple cloning site

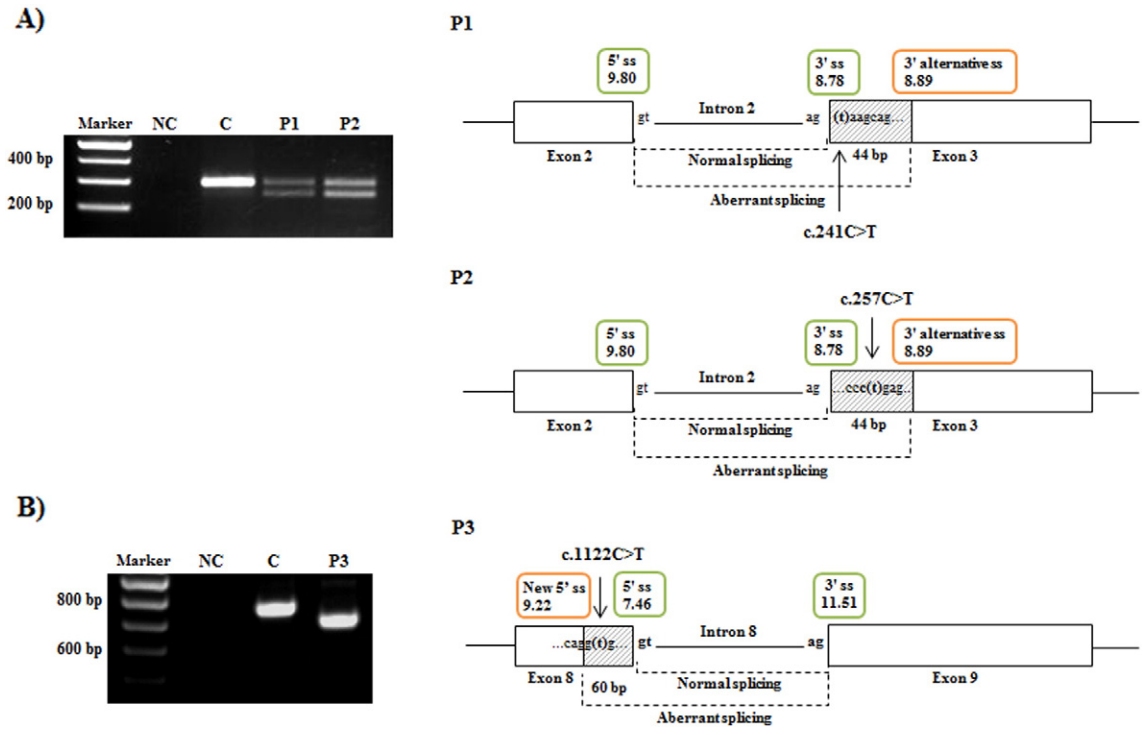

Fig. 1. Agarose gel showing the *IDS* transcripts observed in the three MPS II patients together with schematic views of each transcript's constitution. Sequencing analysis identified the structure of each amplified fragment. The diagrams show the position of the three splicing mutations and its effects on splicing. The splicing scores calculated using *MaxEntScan* software are shown in colored boxes above the corresponding 5′ and 3′ splice sites. A) Negative control (NC); healthy control (C) and Patients 1 (P1) and 2 (P2). Agarose gel electrophoresis after RT-PCR showed one band for the control fibroblasts and two for those of Patients 1 and 2. In both patients the upper band revealed a sequence with exons 2 and 3, with the nucleotide changes c.241C>T (P1) and c.257C>T (P2) in exon 3. The lower band reveals the deletion of the first 44 bp of exon 3 in both patients. B) Negative and healthy control, and Patient 3 (P3). RT-PCR amplification of patient mRNA between exons 7 and 9 revealed an aberrant transcript lacking the last 60 bp of exon 8.

is flanked by functional splice donor and acceptor sites. For this, gene fragments comprising exon 8 and its intronic flanking regions were amplified from the DNA of both control and patient fibroblasts using the primers shown in Table I [34], employing the PCR conditions described above. After subcloning into the TOPO vector, each insert was excised with EcoRI, purified, and cloned into the pSPL3 final vector (Fig. 1C in [34]). All clones were verified by DNA sequencing.

2.7. In vitro splicing assays

The *in vitro* splicing assays were performed in COS-7 and Hep3B cell lines to investigate which one best reproduces the endogenous splicing pattern observed in patients. For that, cells from both lines (4×10^5) were grown in 6-well plates and transfected with WT or mutant minigenes (2 μg) using 4 μl of Lipofectamine 2000 (Invitrogen, Carlsbad, USA) according to the manufacturer's instructions (performed in triplicate). Following the same conditions the mutant minigene (ex3 del ESE/ESS motifs) was transfected in Hep3B cells. At 24 h post-transfection, total RNA was extracted from the cells and used as a template for cDNA synthesis. RT-PCR was then performed as described above, using vector specific pcDNA3.1-myc (K-myc-Bam and pfGHr1) or pSPL3 (SD6 and SA2) primers (Table I in [34]). The amplified products were separated by agarose gel electrophoresis. Following band excision and purification they were subjected to direct sequencing using an ABI Prism 3130xl genetic analyzer (Applied Biosystems, Foster City, USA).

2.8. Overexpression and depletion of splicing factors

To confirm the predicted changes in the splicing factors SRSF2, hnRNP E1 and hnRNP E2, overexpression and depletion studies were performed using plasmids coding for them (kindly provided by Dr. B. Andersen and Dr. S. Liebhaber) and siRNA molecules respectively. Some 4×10^5 Hep3B cells grown in 6-well plates were co-transfected with plasmids encoding the SRSF2, hnRNP E1 or E2 *trans*-acting factors (using 1.5–3.5 μg of each minigene), plus 2 μg of WT or mutant minigenes. All transfections were performed using Lipofectamine 2000 reagent. The amount of plasmid DNA was adjusted as necessary using empty vector (i.e., without any insert). At 48 h post-cotransfection, the cells were harvested and the transcript pattern analyzed by RT-PCR as described above.

Depletion studies were also performed in the Hep3B cell line. Cells at 30–40% confluence were transfected (using Lipofectamine 2000) with siRNA (200 μM) targeting the mRNA of SRSF1 (formerly ASF/SF2) and luciferase (control). These cells were then transfected with the WT or mutant minigene (c.257C>T) 24 h later. RT-PCR analysis was performed 48 h later. All siRNA oligos came from MWG Biotech (Ebersberg, Germany); the sequences are described in Table I [34].

The overexpression of SRSF2 and hnRNP E1 and hnRNP E2 was confirmed in whole cell lysates by quantitative Real-Time PCR (qRT-PCR). Briefly, 1.5 μg of total RNA was reverse-transcribed using NOT *I-d*$(T)_{18}$ bifunctional primer with first-strand mix beads from the Ready-To-Go You-Prime First-Strand Beads Kit (GE Healthcare, Buckinghamshire, UK) according to the manufacturer's protocol. Relative levels of gene expression were analyzed using TaqMan Universal PCR Master Mix 1× (Applied Biosystems) and the TaqMan Gene Expression Kit (which includes primers and probes for each specific splicing factor gene –Table I in [34]), following the recommended PCR conditions.

The relative mRNA levels of target genes were calculated using standard curves (values ranging from 0.05 ng to 50 ng of RNA converted into cDNA). A standard curve was constructed for each target gene relating Ct values (the fractional cycle number at which the amount of amplified target reached a fixed threshold) to log RNA quantities. The normalization of expression was given by the ratio between the RNA concentrations of each target gene and the endogenous gene *PGK1*. The relative amount of RNA was determined via the ratio of the normalized expressions of the target and control samples.

Depletion of SRSF1 was confirmed in whole cell lysates through a qRT-PCR assay as described above and also by Western blotting. For protein analysis, samples were boiled for 10 min and resolved in a 12% SDS-PAGE mini-gel. After electrophoresis, proteins were transferred to a polyvinylidene difluoride membrane using a Mini Trans-Blot cell (Bio-Rad). Immunodetection was carried out using the primary antibodies mouse anti-SF2/ASF clone 96 from Zymed (San Francisco, CA) and anti-α-tubulin from Sigma-Aldrich (Switzerland).

2.9. Antisense oligonucleotide treatment and analysis

AMOs were designed to target the new 5′ splice site created in the presence of the mutation c.1122C>T in exon 8. AMOs were synthesized and purified by Gene Tools (Philomath, OR). A standard 25-mer morpholino control oligonucleotide (also provided by Gene Tools) was used as a negative control (Table I in [34]). Endo-Porter Reagent (Gene Tools) was used as the peptide delivery system, following the manufacturer's recommendations. For the AMO treatment, between 3 and 4×10^5 fibroblasts from control and patient were grown in 6-well plates and after overnight culture different concentrations of each AMO were added with 9 μl/ml of Endo-Porter. The scrape delivery method was also used to help cells incorporate AMOs [39].

To target and block the new 5′ splice site in exon 8, an LNA was designed and synthesized by Exiqon (Vedbaek, Denmark) (Table I in [34]). For LNA exposure, fibroblasts from control and patient were plated under the same conditions as described for AMO treatment. After overnight incubation, different concentrations of LNA were added to cells using Lipofectamine LTX or 2000 (Invitrogen, Carlsbad, USA) as delivery reagents.

After 24 h and 48 h treatment with the different AMOs and LNA, cells were harvested, total mRNA isolated, and RT-PCR performed as described above using the forward and reverse primers for exon 7 and 9 respectively (Table I in [34]).

3. Results

3.1. Genetic analysis of patient-derived fibroblasts

Table 1 shows the genetic defects carried by the patients. Patient 1 was hemizygous for a nucleotide change in exon 3, c.241C>T (p.Q81X) already erroneously reported as p.Q80R by Brusius-Facchin et al. [32]. A detailed analysis of the codon in the HGMD database (Professional 2014.3 Release) showed the mutation reported by these authors was, in fact, Q81X. The impact of this change at the RNA level and its effects on *IDS* pre-mRNA splicing is here addressed for the first time.

Transcriptional analysis of *IDS* cDNA from Patient 1 revealed two transcripts, one corresponding to a normal splicing product with the C>T change in the first nucleotide of exon 3 (predicted to introduce an early stop codon at position 81 [p.Q81X]), and the other corresponding to an aberrant transcript lacking the first 44 bp of exon 3 (predicted to code for a truncated protein with only 83 amino acids) (Fig. 1A). This additional transcript suggests that this point mutation interferes with splicing. Further, since both transcripts bear a premature STOP codon, they are likely targets for nonsense-mediated mRNA decay (NMD), with no protein being produced. When patients' cells were treated with cycloheximide, an inhibitor of the NMD mechanism, a clear increase in the intensity of the band which corresponds to the transcript bearing the nonsense mutation Q81X (Fig. 2) was observed, meaning that this transcript is targeted by NMD. Regarding the abnormal splicing product (with the absence of 44 bp), despite being a potential target for NMD (once leads to a truncated protein, p.Q81EfsX2), no significant changes were observed in the intensity of the corresponding band. The classical NMD pathway is thought to be trigged during the pioneer round of translation when the first ribosome translates the processed mRNA and stalls at a PTC that is located more than 50–55 nucleotides

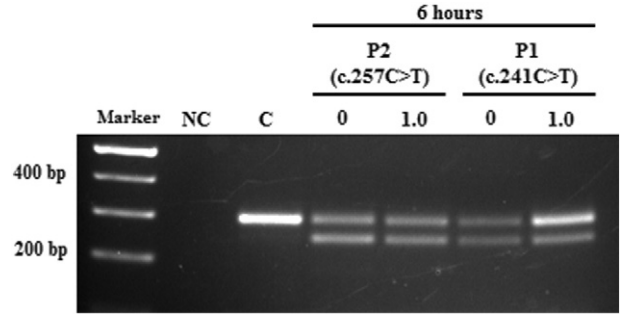

Fig. 2. Cycloheximide treatment. RT-PCR amplification of RNA extracted from mucopolysaccharidosis II patients with the nonsense c.241C>T (P1) and missense c.257C>T (P2) mutations untreated (0 mg/ml) or treated with cycloheximide (1.0 mg/ml) for 6 h. The same results were obtained with 0.75 and 2.0 mg/ml (data not shown). The amplification of a wild-type sample (C) is also presented. NC — negative control; C — control; P — patient; CHX — cycloheximide.

upstream of the last EJC (Exon Junction Complex) [40]. However, there is growing evidence that mutation, codon, gene, cell and tissue-specific differences in NMD efficiency can alter the underlying disease pathology. Moreover, inter-individual variation in NMD efficiency among patients carrying identical mutations have also been reported [41,42]. The differences in the NMD mechanism activation here observed between two transcripts having PTCs could be explained by this recent data.

cDNA analysis was performed for fibroblasts from Patients 2 and 3, who carried mutations already described and previously analyzed in our group [29]. The transcript pattern for Patient 2, who carried the nucleotide change c.257C>T in exon 3, was similar to that observed for Patient 1 (Fig. 1A). Cycloheximide experiments were also performed in this case and, as described for Patient 1, no significant changes in the intensity of the band corresponding to the transcript lacking the 44 bp were observed (Fig. 2). The nucleotide change c.1122C>T carried by Patient 3 (Fig. 1B) was expected to be synonymous in terms of amino acid coding [p.G374G (GGC-GGT)], but the cDNA analysis revealed the presence of a transcript lacking the last 60 bp of exon 8. As previously described [29,30], the normal transcript was also present but in lower quantities. The presence of this transcript even in lower quantities is responsible for the mild phenotype of this patient. In our previous study [29] we have determined patients' enzymatic activities and for this patient we have observed a relatively higher IDS enzymatic activity, in comparison with other MPS II cases.

3.2. Bioinformatic analysis

Splicing scores for the splice site junctions were found compatible with the splicing changes observed in cDNA. For the mutation c.241C>T, *in silico* analysis predicted a reduction in the 3′ splice site score value from 8.78 to 8.13. Under these circumstances the constitutive splice site continued to be used, but the regulation of splicing in this region was perturbed and a downstream cryptic splice site (8.89) was also used, producing a second transcript without the first 44 bp of exon 3 (Fig. 1A). In contrast to what we have observed before [29] for two other *IDS* mutations (c.241−2A>G and c.241−1G>A) which affect the same splice site, in the case of the c.241C>T change the presence of a transcript with the total skipping of the exon 3 was not detected. In fact, the two other mutations affect the 3′ invariable splice site sequence, being responsible for a drastic reduction of the splice site score. That is not the case of c.214C>T change, once this mutation alters the first base of the exon 3, causing only a slightly decrease in the 3′ splice site score (from 8.78 to 8.13) which might explain the aberrant splicing pattern differences observed.

For the c.257C>T mutation, *in silico* analysis returned a higher splicing score for the 3′ cryptic splice site in exon 3 (8.89) than for its constitutive counterpart (8.78) (Fig. 1A).

The change in c.1122C>T was shown to be associated with the activation of a new 5′ splice site in exon 8, which returned a higher splicing score (9.22) than the original splice site (7.46) (Fig. 1B).

Since the *MaxEntScan*-estimated splicing scores did not completely account for the perturbation in constitutive splicing, further bioinformatic tools were used to search for differences in exonic splicing regulatory elements between the WT and mutated sequences of exon 3. For the nucleotide change c.241C>T, neither the *Splicing Rainbow* [38] nor the *ESEfinder* 3.0 [36,37] software's predicted alterations in any exonic splicing regulatory element. In the presence of the c.257C>T nucleotide change, analysis with *Splicing Rainbow* software predicted the elimination of a binding motif for the hnRNP E1 and hnRNP E2 silencing proteins, and the creation of an SRSF1 (formerly ASF/SF2) recognition motif (Fig. 2A in [34]). Analysis with *ESEfinder* 3.0 software indicated the recognition motif for SRSF1 would be slightly altered, and that a binding site for SRSF2 (formerly SC35) would no longer be recognized in the presence of the mutation (Fig. 2B in [34]).

3.3. Functional analysis of IDS gene splicing mutations

To further study the effect of the three exonic changes on splicing patterns, minigene assays were performed using constructs generated with WT or mutant exons (plus their respective intronic flanking regions) in the pcDNA3.1-myc or pSPL3 vectors (Fig. 1A and C in [34]). Fig. 1B and 1D [34] shows the results of RT-PCR splicing analysis after the transfection of COS-7 and Hep3B cells: the amplified transcripts derived from the WT and mutant minigenes are shown in 1B) for the nucleotide changes in exon 3, and in 1D) for the mutation in exon 8.

The transcript patterns for the three *IDS* mutations were similar in both the Hep3B and COS-7 cells, although slight qualitative differences in expression were detected in the minigene assays.

3.4. Splicing regulatory elements analysis

To validate the predictions for the *trans*-acting factor proteins involved in the 3′ splice site choice of *IDS* exon 3, they were either overexpressed or silenced in Hep3B cells transfected with either WT or mutant minigenes constructed for c.257C>T. cDNA analysis after overexpression of the SRSF2 protein in Hep3B cells with the mutant c.257C>T minigene revealed the rescue of the normal transcript and the disappearance of the aberrant form lacking the first 44 nucleotides of exon 3 (Fig. 3B). This strongly suggests that the choice of the 3′ constitutive splice site of *IDS* exon 3 may be dependent on an ESE site recognized by SRSF2. This recognition is compromised by the mutation c.257C>T.

The c.257C>T mutation was further predicted to eliminate a binding motif for the splicing silencers hnRNP E1 and hnRNP E2. The overexpression of hnRNP E1 with the mutant (c.257C>T) minigene resulted in a substantially increased production of the aberrant transcript, showing that the cryptic splice site activated downstream was preferentially chosen (Fig. 3C). This suggests the involvement of hnRNP E1 in the repression of the 3′ constitutive splice site of exon 3. When hnRNP E2 was overexpressed with the mutant (c.257C>T) minigene, no alteration in the mutant splicing pattern was seen (Fig. 3C). Individual co-transfection of SRSF2, hnRNP E1 or hnRNP E2 plus the WT minigene did not modify the WT splicing pattern (Fig. 3A).

Finally, to determine whether the c.257C>T change interfered with the recognition of the splicing enhancer SRSF1, as bioinformatically predicted, endogenous protein in the Hep3B cells was depleted through RNA interference. The cells were then transfected with WT or mutant minigenes. No changes were detected in the transcriptional profiles of either the WT or mutant sequences (Fig. 3D).

The degree of overexpression or suppression achieved for each splicing factor was analyzed by qRT-PCR using specific probes, and by Western blotting in the case of SRSF1 depletion (see Material and Methods). The relative quantification of each RNA, via the ratio of the

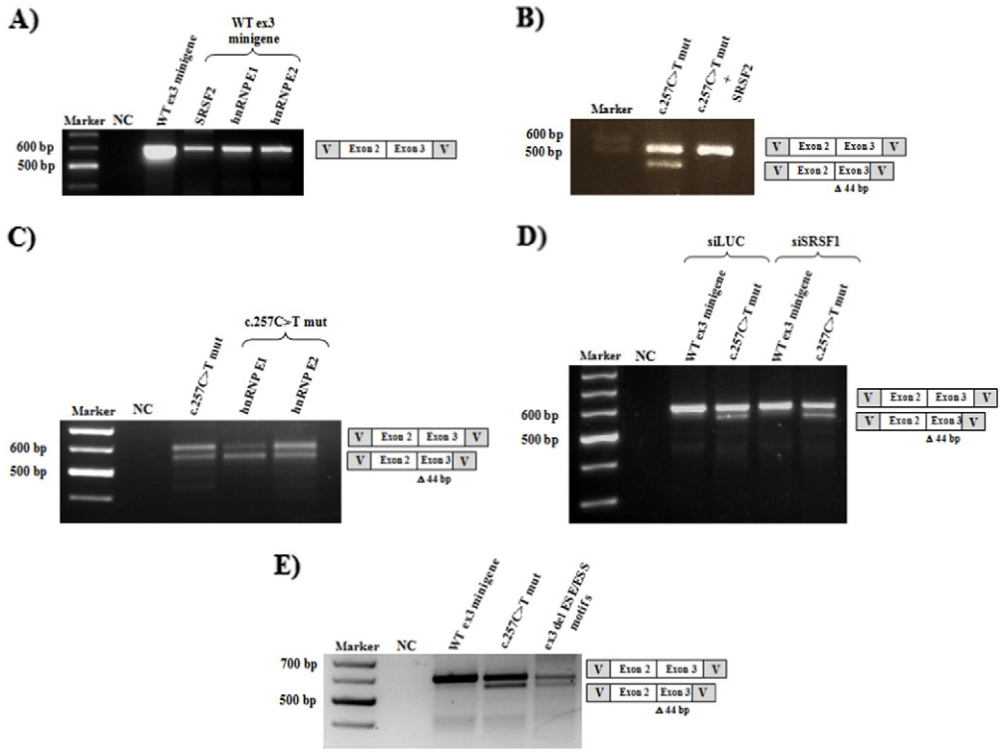

Fig. 3. Analysis of the involvement of specific SR and hnRNP *trans-acting* factors in the regulation of the 3′ splice site of exon 3. The results of RT-PCR analysis using vector-specific primers are shown along with a diagram of the transcripts obtained in Hep3B cells after 24 h or 48 h of incubation. A) Co-transfection of the wild-type exon 3 minigene (2 μg) with each *trans-acting* factor (3.5 μg). B) Overexpression of SRSF2 (formerly SC35) (3.5 μg) after transfection with the c.257C>T mutant minigene (2 μg). C) RT-PCR analysis of processed transcripts after co-transfection with hnRNP E1 or hnRNP E2 (3.5 μg) plus the mutant minigene c.257C>T (2 μg). D) Splicing pattern of the minigene reporter transcripts following depletion of endogenous SRSF1 (formerly ASF/SF2) and luciferase (control). For the silencing of both proteins, 200 μM of each siRNA were used. Note that only the SRSF2 and hnRNP E1 *trans*-acting proteins had an effect (respectively) on the constitutive and alternative splicing of *IDS* exon 3. The same results were obtained when between 1.5 μg and 3 μg of the *trans*-acting factors were overexpressed. E) Transcript pattern obtained after expression of 2 μg of the exon 3 mutant minigene (ex3 del ESE/ESS motifs) with the deletion of 6 bp (GCCCCGAGCC) of predicted exonic motifs with overlapping sequences for the binding of SRSF2 and hnRNP E1 and hnRNP E2 proteins. NC — negative control; V — vector sequence; siRNA — small interfering RNA.

normalized expressions of the target and control samples, confirmed the efficacy of SRSF2, hnRNP E1 and hnRNP E2 overexpression, as well as SRSF1 depletion (Table II in [34]). SRSF1 depletion was also confirmed by immunodetection (Fig. 3 in [34]).

The expression in Hep3B cells of the mutant minigene (ex3 del ESE/ESS motifs) containing the deletion of 6 bp (GCCCCGAGCC) of the predicted *cis*-acting motifs for the binding of SRSF2 and hnRNP E1 and E2 showed the aberrant splicing pattern observed in the presence of the c.257C>T mutation (Fig. 3E). This result, as the ones obtained with the overexpression of SRSF2 and hnRNP E1 proteins, points to the involvement of these two *trans*-acting factors in the regulation of the 3′ constitutive splice site of *IDS* exon 3.

3.5. Antisense oligonucleotide studies in control and patient fibroblasts with the mutation c.1122C>T in IDS gene: a therapeutic approach

Given that the mutation c.1122C>T in exon 8 has a silent effect on the amino acid sequence, the possibility of redirecting transcript processing using modified antisense oligonucleotides of two different types was examined. Three AMOs and one LNA complementary to the region of the newly created 5′ splice site (Fig. 4A) were designed in an attempt to block the access of the splicing machinery to the mutant pre-mRNA, and consequently circumvent the formation of the aberrantly spliced transcript. cDNA analysis was performed 24 h and 48 h after transfection of the patient and control fibroblasts. In patients' fibroblasts, under none of conditions tested (30 or 50 μM of each AMO, and 1, 5, 25, 50 or 100 nM of LNA) was the abnormally spliced mRNA ever abolished. The RT-PCR results (Fig. 4B and C) also showed a transcript skipping exon 8 in the presence of the different AOs, alongside the abnormal transcript showing partial skipping of exon 8. In control fibroblasts transfected with 50 μM of each AMO, the RT-PCR results revealed three different transcripts: one of normal molecular weight, one lacking the last 60 bp of exon 8 and one with the total skipping of exon 8. On the other hand, the transfection of 50 and 100 nM of LNA lead to the appearance of one aberrant transcript presenting the total skipping of exon 8 (Fig. 4D).

The AMO treatment proved to be sequence-specific since an AMO with a scrambled sequence had no effect on the exon 8 splicing pattern in patient fibroblasts (data not shown).

4. Discussion

A number of diseases have been linked to mutations that disrupt the splicing process, which leads to abnormal and/or deficient protein production [9,43]. Splicing defects represent more than 9% of all currently published mutations [6], although this figure might well be underestimated since our knowledge on the regulatory elements that influence splicing in many genes is far from complete. Genomic DNA and cDNA analyses (including functional studies addressing the effect of specific mutations on splicing) are needed if we are to develop therapeutic strategies for correcting molecular defects. In the present work, one of the mutations causing aberrant splicing was a synonymous substitution. This led us to explore the possible use of antisense oligonucleotide therapy for redirecting abnormal pre-mRNA splicing.

Under physiological conditions, the *IDS* gene is associated with at least 8 transcripts produced by alternative splicing (Vega Genome Browser; VEGA: http://vega.sanger.ac.uk/), four of them are protein coding, two are thought to undergo NMD and the last two are processed

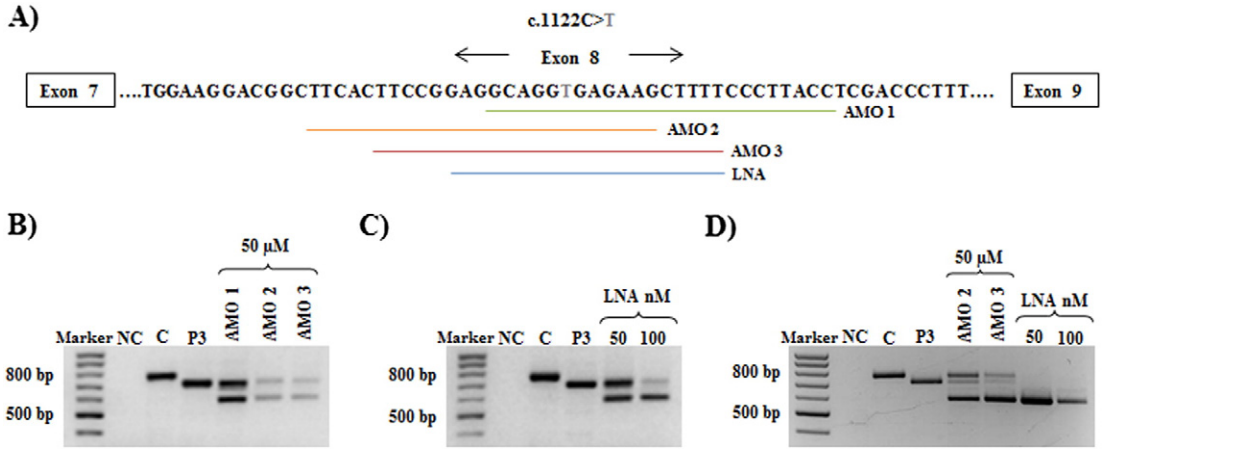

Fig. 4. Antisense oligonucleotide treatment of control and patient fibroblasts. A) Illustration of the *IDS* exon 8 region where the nucleotide change c.1122C>T is located (T change marked in bold gray). The underlined sequences represent each blocking AMO or LNA. B) RT-PCR analysis of mRNA from untreated control cells (C) and from Patient 3 (P3) fibroblasts (0 µM), as well as from P3 cells treated for 24 h with 50 µM of AMO 1, 2 or 3 targeting the new 5′ splice site. C) Same analysis as in B but performed for P3 cells treated for 24 h with 50 and 100 nM of the specific LNA. D) cDNA analysis of control fibroblasts after treatment with 50 µM of AMOs or 50 and 100 nM of LNA. Samples of untreated control (C) and P3 fibroblasts are also presented. The same results were obtained after 48 h of treatment with the three AMOs and LNA (data not shown). NC — negative control.

transcripts that do not have an ORF. This number of transcripts suggests a complex underlying regulatory mechanism that probably requires the interaction of multiple splicing factors. This, of course, also renders this system sensitive to mutations that disrupt splicing. Regulatory sequence elements act *in vivo* as binding sites for specific SR and hnRNP *trans*-acting factors that, respectively, promote and inhibit splice site recognition and spliceosome assembly around a given exon. hnRNPs can disturb the protein-protein interactions of SR proteins, and thus compete with them in splice site recognition [11,44].

For the three disease-causing mutations analyzed in the present work, the *in vitro* splicing analysis of specific minigenes closely reproduced the pattern seen in patient fibroblasts. Therefore, the *cis* and *trans*-acting elements involved in exon 3 splicing regulation were examined in further studies.

The c.257C>T mutation seemed to abolish the exonic splicing enhancer (ESE) for the SRSF2 (formerly SC35) protein, which is predicted to be necessary for the constitutive transcription of exon 3 in the WT context. The overexpression of this SR protein along with the mutant minigene compensated for the aberrant splicing by favoring the selection of the constitutive 3′ splice site by the splicing machinery. In agreement, the *MaxEntScan* splicing score for the 3′ constitutive splice site (8.78) was lower than for the cryptic site situated downstream (8.89). All these findings are consistent with the documented model for ESE function, in which ESE-bound SR proteins are thought to activate weak 3′ splice sites by increasing the recruitment of $U2AF^{65/35}$ and improving its binding stabilization via protein-protein interactions between the SR protein and the $U2AF^{35}$ RS domains [45,46].

The c.257C>T mutation was further predicted to eliminate a binding site for the splicing silencers hnRNP E1 and hnRNP E2; this site overlaps with the interrupted sequence motif for SRSF2 recognition (Fig. 2A in [34]). Overexpression of the hnRNP E1 factor with the mutant minigene resulted in the increased expression of the aberrant transcript, showing that this *trans*-acting factor, which has been reported as a splicing regulator [47-49], may indeed inhibit the recognition of the 3′ constitutive splice site, thus favoring abnormal alternative splicing. Moreover, the transfection of Hep3B cells with a mutant minigene (ex3 del ESE/ESS motifs) presenting the deletion of a 6 bp sequence (CCCGAG) which comprises the predicted *cis*-acting motifs for the binding of SRSF2 and hnRNP E1 lead also to the appearance of the aberrant splicing product with the absence of the 44 bp. This observation further supports the hypothesis that this region contains important *cis*-acting elements for the regulation of the 3′ splice site of exon 3.

The *in vitro* expression or silencing of splicing factors can modulate splicing patterns, revealing that precise combinations and relative ratios of factors dictate regulatory decisions [10,50]. Overall, the present results suggest that the binding of hnRNP E1 to exon 3 can modulate the interaction of SRSF2 with an overlapping site (Fig. 5). The mutant minigene analysis together with the overexpression data for both proteins indicate that SRSF2 binding to the ESE seems to be important for splicing of the upstream intron, and that it might depend on changes in the concentration ratio between the SR protein and hnRNP E1. Further, and notably, the overexpression of hnRNP E1 via the WT minigene showed no alteration of the normal splicing pattern; thus, an excess of hnRNP E1 may be insufficient to antagonize the binding of SRSF2 and disturb constitutive splicing. This suggests that differences in the concentrations of these RNA-binding proteins may be required for exon 3 to be silenced by hnRNP E1. A similar occlusion model involving the hnRNP A1 and SRSF2 protein splicing factors has been described in which the function of hnRNP in *tat* exon 2 splicing was to inhibit the binding of SRSF2 to an overlapping site [51,52]. The ability of hnRNPs to interfere with the binding of SR proteins has also been described in other pre-mRNAs [53-55].

hnRNP E1 and hnRNP E2 are highly homologous proteins, with 89% amino acid similarity [56]. Nonetheless, the overexpression of hnRNP E2 with the WT and mutant constructs did not alter the splicing pattern. This shows that, despite being very alike, they may recognize different sequence motifs. Distinct functions for these proteins have been reported by other authors [49,57].

As a whole, these findings contribute towards our better understanding of the molecular splicing mechanism of *IDS*. The results, like others reported for disease-related mutations [58-61], are of importance for clarifying the basic mechanisms underlying *IDS*-associated splicing, but improve our knowledge of the splicing process in general. This is a prerequisite for the design of new gene-specific therapeutic strategies.

This study also examined whether the aberrant splicing effect produced by the synonymous mutation c.1122C>T in *IDS* exon 8 could be neutralized via the use of specific antisense oligonucleotides. In patient cells, assays were performed with different AMOs and an LNA designed to bind to different sites around the new donor splice site. However, the abnormal transcript was still produced, and a new transcript skipping exon 8 was induced. This total absence of exon 8 led to the in-frame loss of 58 amino acids instead of the 20 lost through the absence of the last 60 nucleotides of exon 8. In addition, the skipping of

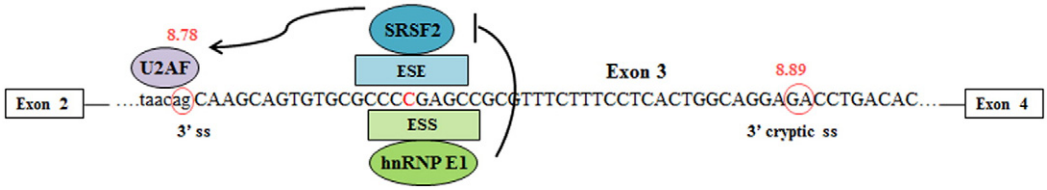

Fig. 5. Hypothetical model for the regulation of the constitutive splicing mechanism around the 3′ splice site of *IDS* exon 3. Exon 3 contains an exonic splicing silencer (ESS) motif recognized by hnRNP E1 that overlaps with an exonic splicing enhancer (ESE) element bound by SRSF2 (formerly SC35). Both the ESE and ESS motifs are eliminated by the c.257C>T mutation. SRSF2 overexpression can rescue the use of the 3′ splice site while hnRNP E1 overexpression increases the use of the downstream cryptic splice site.

exon 8 (recorded at the cDNA level) has been reported to be disease-causing in one patient [62]. Thus, the induction of this transcript would be of no therapeutic use.

Although the tested AOs fulfilled most of the criteria for efficacy, none of them directed exon 8 splicing towards correction. This shows that even though an AO strategy may be appropriately designed, there is no guarantee of success. Negative results have been obtained for 50% (17 of 34) of the AOs designed to inhibit *ICAM-1* expression [63], and 33% (52 of 156) of a series of exon-internal AOs designed to induce exon skipping in the dystrophin gene [64] failed to have the desired effect. Problems of target accessibility caused by the secondary or tertiary mRNA structure, and/or by proteins bound to it, might account for some failures of oligonucleotides [65]. Further, short LNA oligonucleotides (16-mer or even 12-mer) are known to be more specific and effective. The size of the LNA used (20-mer) in the present work, might, therefore explain (at least partly) its lack of effectiveness. It was not possible to use a shorter oligonucleotide to specifically block the region of the new "gt" donor splice site due to the lack of gene specificity of <20-mer sequences; this would certainly derail any attempt at therapy.

It might be thought that the different oligonucleotides obstruct the access of specific SR proteins to their respective ESE binding motifs, thus promoting the skipping of exon 8 [66]. Such a scenario is also predicted by the *in silico* analysis results (summarized in Table 2), which indicate exon 8 to contain a region where AO binding occurs, in which distinct binding motifs are likely present at different positions. This prediction is supported by the results of the AMOs and LNA transfection in control fibroblasts wherein the splicing pattern is changed towards to aberrant forms (including exon 8 skipping), pointing to an important role of the predicted exonic binding motifs in the 5′ splice site regulation of exon 8. In addition, since two of the alternative *IDS* transcripts lack exon 8 (www.ensembl.org), regulation around this exon may be rather complex, compromising the efficacy of the AOs assayed. Studies are required to explore the use of oligonucleotides designed to bind to other regions of exon 8; an oligonucleotide distant from the mutation might have a positive effect on the retention of exon 8, helping more effective solutions for exon 8 recovery to be designed. Until then we should be careful in consider definitively that an antisense therapeutic strategy is not applicable to the splicing rescue of this mutation. Nevertheless, and as is highlighted by the present study, one such approach may be particularly challenging for this region of the *IDS* gene.

Since antisense therapy is mutation-targeted, and the target defects usually involve 'private' mutations (i.e., they affect only one person and his or her family members), it can be understood as personalized medicine. Efforts are currently underway to allow AOs to be regarded as a single drug class; this could dramatically accelerate progress in the development of antisense drug therapies for RNA mis-splicing diseases [67,68].

To our knowledge this is the first attempt to modulate an MPS II-causing splicing mutation using antisense oligonucleotides. Although little success was enjoyed, the results raise new questions regarding the use of antisense therapy in diseases involving finely regulated gene systems.

Table 2
In silico prediction of the effect of exonic splicing enhancer (ESE) binding motifs on the *IDS* exon 8 mutant sequence (c.1122C>T) using *ESR*search (http://ibis.tau.ac.il/ssat/ESR.htm) [69], *RESCUE-ESE* (http://genes.mit.edu/burgelab/rescue-ese/) [70] and *ESEfinder* 3.0 (http://rulai.cshl.edu/cgi-bin/tools/ESE3/esefinder.cgi?process=home) [36,37] software. Each column shows the ESE binding motifs present in the mutant exon 8 region where antisense oligonucleotides (AOs) binding occurs. Number of base pairs of exon 8 = 174 bp. The AO binding region lies between nucleotides 97 and 134. Numbers in brackets refer to the first nucleotide position of the predicted binding motif.

IDS exon 8 sequence	*ESR*search	*RESCUE-ESE*	*ESEfinder* 3.0
SR protein binding motifs	TTCCGG (103) TGAGAAGCTT (116) TGAGAAGC (116) GAGAAG (117) TACCTC (132)	TGAGAA (116) GAGAAG (117) AGAAGC (118)	GGCAGGT (110)

Transparency document

The Transparency document associated with this article can be found in the online version.

Acknowledgments

LM was supported by a grant (SFRH/BD/64592/2009) from the *Fundação para a Ciência e Tecnologia IP* (FCT)/POPH/FSE, Portugal.

Research involving human participants

All procedures performed in studies involving human participants were in accordance with the ethical standards of the institutional and/or national research committee and with the 1964 Helsinki declaration and its later amendments or comparable ethical standards.

Informed consent

Informed consent was obtained from all individual participants included in the study.

Disclosure of potential conflicts of interest

The authors have no conflicts of interest to disclose.

References

[1] E.F. Neufeld, J. Muenzer, Part 12: 78 The Mucopolysaccharidoses, in: C.R. Scriver, A.L. Beaudet, W.S. Sly, D. Valle (Eds.), The Metabolic and Molecular Bases of Inherited Disease, 8th e, vol. II, McGraw-Hill, New York 2001, pp. 2465–2495.

[2] P.J. Wilson, C.P. Morris, D. Anson, T. Occhiodoro, J. Bielicki, P.R. Clements, J.J. Hopwood, Hunter syndrome: isolation of an iduronate-2-sulfatase cDNA clone and analysis of patient DNA, Proc. Natl. Acad. Sci. 87 (1990) 8531–8535.

[3] M.L. Bondeson, H. Malmgren, N. Dahl, B.M. Carlberg, U. Petterson, Presence of an IDS-related locus (IDS2) in Xq28 complicates the mutational analysis of Hunter syndrome, Eur. J. Hum. Genet. 3 (1995) 219–227.

[4] M. Rathmann, S. Bunge, C. Steglich, E. Schwinger, A. Gal, Evidence for an iduronate-sulfatase pseudogene near the functional Hunter syndrome gene in Xq27.3-q28, Hum. Genet. 95 (1995) 34–38.

[5] K.M. Timms, F. Lu, Y. Shen, C.A. Pierson, D.M. Muzny, Y. Gu, D.L. Nelson, R.A. Gibbs, 130 kb of DNA sequence reveals two new genes and a regional duplication distal to the human iduronate-2-sulfate sulfatase locus, Genome Res. 5 (1995) 71–78.

[6] P.D. Stenson, M. Mort, E.V. Ball, K. Shaw, A.D. Phillips, D.N. Cooper, The Human Gene Mutation Database: building a comprehensive mutation repository for clinical and molecular genetics, diagnostic testing and personalized genomic medicine, Hum. Genet. 133 (2014) 1–9.

[7] L. Cartegni, S.L. Chew, A.R. Krainer, Listening to silence and understanding nonsense: exonic mutations that affect splicing, Nat. Rev. Genet. 3 (2002) 285–298.

[8] S. Lualdi, M.G. Pittis, S. Regis, R. Parini, A.E. Allegri, F. Furlan, B. Bembi, M. Filocamo, Multiple cryptic splice sites can be activated by IDS point mutations generating misspliced transcripts, J. Mol. Med. (Berl.) 84 (2006) 692–700.

[9] A.J. Ward, T.A. Cooper, The pathobiology of splicing, J. Pathol. 220 (2010) 152–163.

[10] A.J. Matlin, F. Clark, C.W.J. Smith, Understanding alternative splicing: towards a cellular code, Nat. Rev. Mol. Cell Biol. 6 (2005) 386–398.

[11] Z. Wang, C.B. Burge, Splicing regulation: from a parts list of regulatory elements to an integrated splicing code, RNA 14 (2008) 802–813.

[12] M.A. Havens, M.D. Dominik, M.L. Hastings, Targeting RNA splicing for disease therapy, Wiley Interdiscip. Rev. RNA 4 (3) (2013) 247–266.

[13] B. Pérez, M. Ugarte, L.R. Desviat, V.A. Erdmann, RNA-based therapies for inherited metabolic diseases, in: J. Barciszewski (Ed.), RNA Technologies. From Nucleic Acids Sequences to Molecular Medicine, Springer-Verlag Berlin Heidelberg 2012, pp. 357–370.

[14] R. Kole, A.R. Krainer, S. Altman, RNA therapeutics: beyond RNA interference and antisense oligonucleotides, Nat. Rev. Drug Discov. 11 (2012) 125–140.

[15] B. Pérez, L. Rodríguez-Pascau, L. Vilageliu, D. Grinberg, M. Ugarte, L.R. Desviat, Present and future of antisense therapy for splicing modulation in inherited metabolic disease, J. Inherit. Metab. Dis. 33 (2010) 397–403.

[16] S. Svasti, T. Suwanmanee, S. Fucharoen, H.M. Moulton, M.H. Nelson, N. Maeda, O. Smithies, R. Kole, RNA repair restores hemoglobin expression in IVS2-654 thalassemic mice, Proc. Natl. Acad. Sci. U. S. A. 106 (2009) 1205–1210.

[17] L. Du, J.M. Pollard, R.A. Gatti, Correction of prototypic ATM splicing mutations and aberrant ATM function with antisense morpholino oligonucleotides, Proc. Natl. Acad. Sci. U. S. A. 104 (2007) 6007–6012.

[18] L. Du, R. Kayali, C. Bertoni, F. Fike, H. Hu, P.L. Iversen, R.A. Gatti, Arginine-rich cell-penetrating peptide dramatically enhances AMO-mediated ATM aberrant splicing correction and enables delivery to brain and cerebellum, Hum. Mol. Genet. 20 (2011) 3151–3160.

[19] B. Pérez, G.–.S. LG, A. Verdú, B. Merinero, P. Yuste-Checa, P. Ruíz-Sala, R. Calvo, A. Jalan, L.L. Marín, O. Campos, M.A. Ruíz, M. San Miguel, M. Vázquez, M. Castro, I. Ferrer, R. Navarrete, L. Ruiz-Desviat, P. Lapunzina, M. Ugarte, C. Pérez-Cerdá, Clinical, biochemical, and molecular studies in pyridoxine-dependent epilepsy. Antisense therapy as possible new therapeutic option, Epilepsia 54 (2013) 239–248.

[20] S. Regis, F. Corsolini, S. Grossi, B. Tappino, D.N. Cooper, M. Filocamo, Restoration of the normal splicing pattern of the *PLP1*gene by means of an antisense oligonucleotide directed against an exonic mutation, PLoS One 8 (2013), e73633.

[21] L. Rodríguez-Pascau, M.J. Coll, L. Vilageliu, D. Grinberg, Antisense oligonucleotide treatment for a pseudoexon-generating mutation in the NPC1 gene causing Niemann–Pick type C disease, Hum. Mutat. 30 (2010) E993–E1001.

[22] B. Pérez, A. Rincón, A. Jorge-Finnigan, E. Richard, B. Merinero, M. Ugarte, L.R. Desviat, Pseudoexon exclusion by antisense therapy in methylmalonic aciduria (MMAuria), Hum. Mutat. 30 (2009) 1676–1682.

[23] A. Rincón, C. Aguado, L.R. Desviat, R. Sánchez-Alcudia, M. Ugarte, B. Pérez, Propionic and methylmalonic acidemia: antisense therapeutics for intronic variations causing aberrantly spliced messenger RNA, Am. J. Hum. Genet. 81 (2007) 1262–1270.

[24] Y. Hua, T.A. Vickers, H.L. Okunola, C.F. Bennett, A.R. Krainer, Antisense masking of an hnRNP A1/A2 intronic splicing silencer corrects SMN2 splicing in transgenic mice, Am. J. Hum. Genet. 82 (2008) 834–848.

[25] D.R. Mercatante, C.D. Bortner, J.A. Cidlowski, R. Kole, Modification of alternative splicing of Bcl-x pre-mRNA in prostate and breast cancer cells, J. Biol. Chem. 276 (2001) 16411–16417.

[26] R.V. Giles, D.G. Spiller, R.E. Clark, D.M. Tidd, Antisense morpholino oligonucleotide analog induces missplicing of C-myc mRNA, Antisense Nucleic Acid Drug Dev. 9 (1999) 213–220.

[27] H.S. Sekhon, C.A. London, M. Sekhon, P.L. Iversen, G.R. Devi, c-MYC antisense phosphorodiamidate morpholino oligomer inhibits lung metastasis in a murine tumor model, Lung Cancer 60 (2008) 347–354.

[28] T. Koo, M.J. Wood, Clinical trials using antisense oligonucleotides in Duchenne muscular dystrophy, Hum. Gene Ther. 24 (2013) 479–488.

[29] S. Alves, M. Mangas, M.J. Prata, G. Ribeiro, L. Lopes, H. Ribeiro, J. Pinto-Basto, M.R. Lima, L. Lacerda, Molecular characterization of Portuguese patients with mucopolysaccharidosis type II shows evidence that the IDS gene is prone to splicing mutations, J. Inherit. Metab. Dis. 29 (2006) 743–754.

[30] S. Bunge, C. Steglich, C. Zuther, M. Beck, C.P. Morris, E. Schwinger, A. Schinzel, J.J. Hopwood, A. Gal, Iduronate-2-sulfatase gene mutations in 16 patients with mucopolysaccharidosis type II (Hunter syndrome), Hum. Mol. Genet. 2 (1993) 1871–1875.

[31] R.H. Flomen, P.M. Green, D.R. Bentley, F. Giannelli, E.P. Green, Detection of point mutations and a gross deletion in six hunter syndrome patients, Genomics 13 (1992) 543–550.

[32] A.C. Brusius-Facchin, S. Iv, C. Zimmer, M.G. Ribeiro, A.X. Acosta, D. Horovitz, I.L. Monlleó, M.I. Fontes, A. Fett-Conte, R.P. Sobrinho, A.R. Duarte, R. Boy, P. Mabe, M. Ascurra, M. de Michelena, K.L. Tylee, G.T.N. Besley, M.C.V. Garreton, R. Giugliani, S. Leistner-Segal, Mucopolysaccharidosis type II: identification of 30 novel mutations among Latin American patients, Mol. Genet. Metab. 111 (2014) 133–138.

[33] E. Popowska, M. Rathmann, A. Tylki-Szymanska, S. Bunge, C. Steglich, E. Schwinger, A. Gal, Mutations of the iduronate-2-sulfatase gene in 12 Polish patients with mucopolysaccharidosis type II (Hunter syndrome), Hum. Mutat. 5 (1995) 97–100.

[34] L. Matos, V. Gonçalves, E. Pinto, F. Laranjeira, M.J. Prata, P. Jordan, L.R. Desviat, B. Pérez, S. Alves, Data in support of a functional analysis of splicing mutations in the *IDS* gene and the use of antisense oligonucleotides to exploit an alternative therapy for MPS II, Data Brief (2015) Submitted.

[35] G. Yeo, C.B. Burge, Maximum entropy modeling of short sequence motifs with applications to RNA splicing signals, J. Comput. Biol. 11 (2004) 377–394.

[36] L. Cartegni, J. Wang, Z. Zhu, M.Q. Zhang, A.R. Krainer, ESEfinder: a web resource to identify exonic splicing enhancers, Nucleic Acids Res. 31 (2003) 3568–3571.

[37] P.J. Smith, C. Zhang, J. Wang, S.L. Chew, M.Q. Zhang, A.R. Krainer, An increased specificity score matrix for the prediction of SF2/ASF-specific exonic splicing enhancers, Hum. Mol. Genet. 15 (2006) 2490–2508.

[38] S. Stamm, J.J. Riethoven, V. Le Texier, C. Gopalakrishnan, V. Kumanduri, Y. Tang, N.L. Barbosa-Morais, T.A. Thanaraj, ASD: a bioinformatics resource on alternative splicing, Nucleic Acids Res. 34 (2006) D46–D55.

[39] M. Partridge, A. Vincent, P. Matthews, J. Puma, D. Stein, J. Summerton, A simple method for delivering morpholino antisense oligos into the cytoplasm of cells, Antisense Nucleic Acid Drug Dev. 6 (1996) 169–175.

[40] J.N. Miller, D.A. Pearce, Nonsense-mediated decay in genetic disease: friend or foe? Mutat. Res. Rev. Mutat. Res. 762 (2014) 52–64.

[41] L.S. Nguyen, M.F. Wilkinson, J. Gecz, Nonsense-mediated mRNA decay: inter-individual variability and human disease, Neurosci. Biobehav. 46 (2014) 175–186.

[42] C. Seoighe, C. Gehring, Heritability in the efficiency of nonsense-mediated mRNA decay in humans, PLoS ONE 5 (2010), e11657.

[43] M.A. Lewandowska, The missing puzzle piece: splicing mutations, Int. J. Clin. Exp. Pathol. 6 (2013) 2675–2682.

[44] A. Busch, K.J. Hertel, Evolution of SR protein and hnRNP splicing regulatory factors, Wiley Interdiscip. Rev. RNA 3 (2012) 1–12.

[45] B.R. Graveley, K.J. Hertel, T. Maniatis, The role of $U2AF^{35}$ and $U2AF^{65}$ in enhancer-dependent splicing, RNA 7 (2001) 806–818.

[46] P. Zuo, T. Maniatis, The splicing factor U2AF35 mediates critical protein-protein interactions in constitutive and enhancer-dependent splicing, Genes Dev. 10 (1996) 1356–1368.

[47] S.A. Akker, S. Misra, S. Aslam, E.L. Morgan, P.J. Smith, B. Khoo, S.L. Chew, Pre-spliceosomal binding of U1 small nuclear ribonucleoprotein (RNP) and heterogeneous nuclear E1 is associated with suppression of a growth hormone receptor pseudoexon, Mol. Endocrinol. 21 (2007) 2529–2540.

[48] Q. Meng, S.K. Rayala, A.E. Gururaj, A.H. Talukder, B.W. O'Malley, R. Kumar, Signaling-dependent and coordinated regulation of transcription, splicing, and translation resides in a single coregulator, PCBP1, Proc. Natl. Acad. Sci. U. S. A. 104 (2007) 5866–5871.

[49] K. Woolaway, K. Asai, A. Emili, A. Cochrane, hnRNP E1 and E2 have distinct roles in modulating HIV-I gene expression, Retrovirology 4 (2007) 28.

[50] J.F. Cáceres, A.R. Kornblihtt, Alternative splicing: multiple control mechanisms and involvement in human disease, Trends Genet. 18 (2002) 186–193.

[51] R. Martinez-Contreras, P. Cloutier, L. Shkreta, J.-F. Fisette, T. Revil, B. Chabot, Chapter 8: hnRNP proteins and splicing control, in: B.J. Blencowe, B.R. Graveley (Eds.), Alternative Splicing in the Postgenomic era, Advances in experimental medicine and biology series, vol. 623, Landes Bioscience, New York 2007, pp. 123–147.

[52] A.M. Zahler, C.K. Damgaard, J. Kjems, M. Caputi, SC35 and heterogeneous nuclear ribonucleoprotein A/B proteins bind to a juxtaposed exonic splicing enhancer/exonic splicing silencer element to regulate HIV-1 *tat* exon 2 splicing, J. Biol. Chem. 279 (2004) 10077–10084.

[53] J.B. Crawford, J.G. Patton, Activation of α-tropomyosin exon 2 is regulated by the SR protein 9G8 and heterogeneous nuclear ribonucleoproteins H and F, Mol. Cell. Biol. 26 (2006) 8791–8802.

[54] A.J. Pollard, A.R. Krainer, S.C. Robson, N.G. Europe-Finner, Alternative splicing of the adenylyl cyclase stimulatory G-protein $G\alpha_s$ is regulated by SF2/ASF and heterogeneous nuclear ribonucleoprotein A1 (hnRNPA1) and involves the use of an unusual TG 3′-splice site, J. Biol. Chem. 277 (2002) 15241–15251.

[55] J. Zhu, A. Mayeda, A.R. Krainer, Exon identity established through differential antagonism between exonic splicing silencer-bound hnRNP A1 and enhancer-bound SR proteins, Mol. Cell 8 (2001) 1351–1361.

[56] A. Chaudhury, P. Chander, P.H. Howe, Heterogeneous nuclear ribonucleoproteins (hnRNPs) in cellular processes: focus on hnRNP E1's multifunctional regulatory roles, RNA 16 (2010) 1449–1462.

[57] Y. Zhu, Y. Sun, X.O. Mao, K.L. Jin, D.A. Greenberg, Expression of poly(C)-binding proteins is differentially regulated by hypoxia and ischemia in cortical neurons, Neuroscience 110 (2002) 191–198.

[58] L. Cartegni, M.L. Hastings, J.A. Calarco, E. de Stanchina, A.R. Krainer, Determinants of exon 7 splicing in the spinal muscular atrophy genes, SMN1 and SMN2, Am. J. Hum. Genet. 78 (2006) 63–77.

[59] V. Gonçalves, P. Theisen, O. Antunes, A. Medeira, J.S. Ramos, P. Jordan, G. Isidro, A missense mutation in the APC tumor suppressor gene disrupts an ASF/SF2 splicing enhancer motif and causes pathogenic skipping of exon 14, Mutat. Res. 662 (2009) 33–36.

[60] A.J. Richards, A. McNinch, B. Whitakker Treacy, K. Oakhill, A. Poulson, M.P. Snead, Splicing analysis of unclassified variants in COL2A1 and COL11A1 identifies deep intronic pathogenic mutations, Eur. J. Hum. Genet. 20 (2012) 552–558.

[61] G. Ulzi, V.A. Sansone, F. Magri, S. Corti, N. Bresolin, G.P. Comi, S. Lucchiari, In vitro analysis of splice site mutations in the CLCN1 gene using the minigene assay, Mol. Biol. Rep. 41 (2014) 2865–2874.

[62] V. Ricci, S. Regis, M. Di Duca, M. Filocamo, An Alu-mediated rearrangement as cause of exon skipping in Hunter disease, Hum. Genet. 112 (2003) 419–425.
[63] V. Patzel, U. Steidl, R. Kronenwett, R. Haas, G. Sczakiel, A theoretical approach to select effective antisense oligodeoxyribonucleotides at high statistical probability, Nucleic Acids Res. 27 (1999) 4328–4334.
[64] A. Aartsma-Rus, L. van Vliet, M. Hirschi, A.A. Janson, H. Heemskerk, C.L. de Winter, S. de Kimpe, J.C. van Deutekom, P.A. 't Hoen, G.J. van Ommen, Guidelines for antisense oligonucleotide design and insight into splice-modulating mechanisms, Mol. Ther. 17 (2009) 548–553.
[65] A. Dias, C.A. Stein, Antisense oligonucleotides: basic concepts and mechanisms, Mol. Cancer Ther. 1 (2002) 347–355.
[66] J.C. Long, J.F. Caceres, The SR protein family of splicing factors: master regulators of gene expression, Biochem. J. 417 (2009) 15–27.
[67] S.M. Hammond, M.J. Wood, Genetic therapies for RNA mis-splicing diseases, Trends Genet. 27 (2011) 196–205.
[68] J.A.J. Lee, T. Yokota, Antisense therapy in neurology, J. Perspect. Med. 3 (2013) 144–176.
[69] A. Goren, O. Ram, M. Amit, H. Keren, G. Lev-Maor, I. Vig, T. Pupko, G. Ast, Comparative analysis identifies exonic splicing regulatory sequences —the complex definition of enhancers and silencers, Mol. Cell 22 (2006) 769–781.
[70] W.G. Fairbrother, R.F. Yeh, P.A. Sharp, C.B. Burge, Predictive identification of exonic splicing enhancers in human genes, Science 297 (2002) 1007–1013.